NUMERICAL SIMULATION FOR THE SACRIFICIAL RELEASE OF MEMS SQUARE DIAPHRAGMS

Wen J. Li[1], Jack C. Shih[2], John D. Mai[2], and Chih-Ming Ho[2]
[1]*Department of Mechanical and Automation Engineering, The Chinese University of Hong Kong*
[2]*Department of Mechanical and Aerospace Engineering, University of California, Los Angeles*
Jianqiang Liu[3] and Yu-Chong Tai[4]
[3]*GE Corporate Research & Development, Schenectady, New York*
[4]*Department of Electrical Engineering, California Institute of Technology*

ABSTRACT

Chemical etching of sacrificial layers is a widely used technique in surface micromachining. Etch rate prediction of the sacrificial layer in an etchant is critical for optimizing a giving fabrication process. This paper presents a moving-boundary numerical scheme to predict the motion of a hydrofluoric (HF) acid and phosphosilicate-glass (PSG) etching interface. Results showed the prediction of the etch front propagation for square structures is universally possible for HF concentrations ranging from 3 to 49%. In the process, some physical mechanisms governing the HF-PSG etching phenomenon were elucidated. The results also indicate that the moving-boundary scheme can be extended to predict the etch rate of more complex geometries.

Keywords: sacrificial-etching, surface-micromachining, HF-PSG, MEMS-diaphragm, etching-model.

INTRODUCTION

Chemical etching of sacrificial layers is a widely used technique in surface micromachining to fabricate MEMS devices such as gears[1], hinges[2], and pressure sensors[3]. For example, silicon dioxide (SiO_2) or PSG can be easily etched in HF-based solutions with very high selectivity over silicon (Si) and silicon nitride (Si_2N_3). In fact, etching of SiO_2 in HF was studied as early as 1913[4]. Readily, many chemical models as well as calibrated etching rates of differently doped oxides in HF are available[5,6,7,8]. However, these results only apply to etching experiments intentionally designed to be in the reaction-limited regimes. They are useful when the etching dimensions of the sacrificial layer is <100μm, thus reactive chemicals can always be sufficiently supplied at the etching front, and no diffusion of reactive chemicals is need to sustain the etching mechanism. Therefore, etch time can often be predicted by using the reaction-limited etching rate, which is constant since the HF concentration at the etch front will remain very consistent. In the case of sacrificial layer dimensions >100μm, depletion of reactive chemicals at the etching front occurs, and the etching rate is then dominated by a diffusion mechanism. Consequently a good etch rate prediction model needs to include both chemical reaction and diffusion. In addition, such a model should also be applicable to a wide range of concentration.

Monk et al.[9,10] reported the first study of PSG etching in microchannels using HF-based solutions. Both Deal-Grove and non-first-order models have been examined. It was shown that under specific concentrations both models could fit etching data well. However, no information on the applicability of these models over a wide range of HF concentrations was provided. In fact, Liu et al.[11] found that neither model is universal in terms of predicting the etch rate over a wide range of HF concentrations. An analytical solution was then developed by Liu et al. to universally predict the etch rate of PSG in HF concentrations from 3.0% to 49.0% for straight channels. In their study, an analytical solution was made possible by the assumption of 1-D HF-PSG interface etch front propagation, i.e., the etch rate did not depend on the channel width.

We have developed a technique to extend the results of Liu et al. to predict the etch rate of PSG in HF for other geometries. Specifically, the 2-D interface propagation for a square structure was universally predicted for HF concentrations of 3.0% to 49.0% using a numerical model. In the process, some physical mechanisms governing the HF-PSG etching phenomenon were elucidated. It was also found that the reaction and diffusion constants obtained by Liu et al. can be used to predict the etch rate of more complex geometries.

FABRICATION OF THE TEST STRUCTURES

The test chips were fabricated at Caltech using exactly the same process developed by Liu et al. A layer of 1μm thick LPCVD PSG was deposited at 450°C onto 4" Si wafers. The PSG layer was than densified by thermal annealing at 1000°C for one hour. Many different geometries which include straight channels, square slabs, and other geometric shapes were then patterned onto the PSG layer (Figure 1). This is followed by the deposition of a 1.2μm layer of LPCVD low stress silicon nitride at 820°C. Finally, etching windows are opened using SF_6 plasma. The sacrificial PSG layer has

a phosphorus concentration of 6%. The uniformity of the PSG across the wafer is about ±5%. A cross-sectional view of a representative structure is shown in Figure 2a. Experiments from Liu et al. showed that the straight channel etch rate may be affected by PSG thickness, hence, second generation chips were fabricated by depositing a 1.2μm layer of LPCVD low stress silicon nitride at 820°C on top of the silicon wafers (Figure 2b). The extra layer of silicon nitride was added to protect the silicon substrate layer from HF etching, which was postulated to have affected the etch rate in channels of various thicknesses.

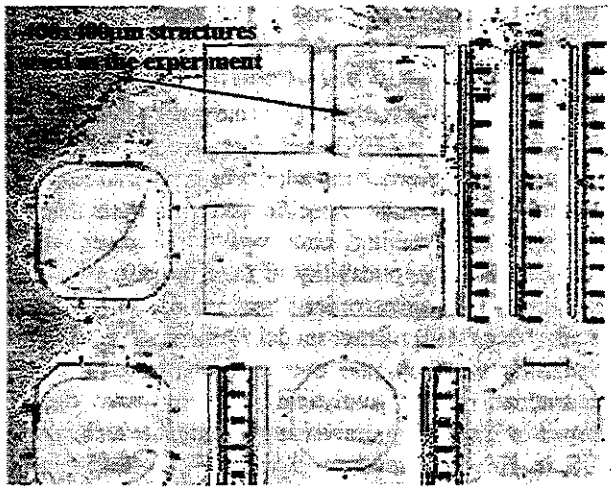

Figure 1: *Some of the structures fabricated for the etch rate prediction experiment. The sacrificial layer is PSG of various thicknesses and the diaphragm material is 1 μm thick Si_2N_3. The square structures are 400×400 μm.*

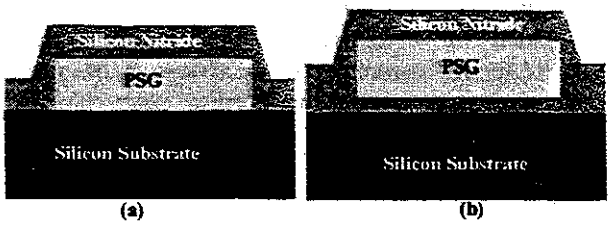

Figure 2: *Cross-sectional view of the test structures. (a) The first generation chip. (b) The second generation chips which have a layer of Si_2N_3 below the PSG layer.*

EXPERIMENTAL SETUP

Similar to the experimental setup of Liu et al., the etching experiments were carried out under an in-situ monitoring system that is illustrated in Figure 3. This monitoring system consists of a microscope, a CCD camera, and a VCR tape recorder. Etching of the chip is performed in a specially designed polypropylene container with a glass cover. The test chip is fixed inside the container by polypropylene clips. Without the clips, bubbles that formed underneath the test chip will tilt the chip, causing the microscope image to become unfocused, making etch rate measurements

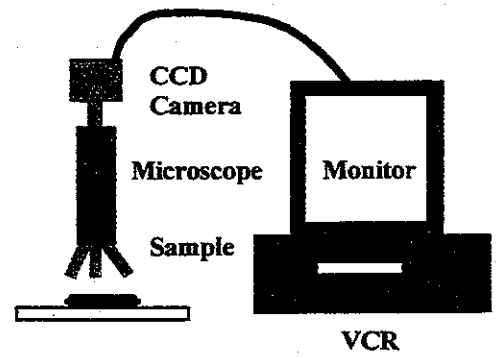

Figure 3: *Sketch of the in-situ monitoring system used to obtain etch rate data.*

inaccurate. A clear transparent glass cover was used to prevent HF fumes from damaging the microscopic lens and diffusing into the ambient air.

ETCH RATE PREDICTION BY NUMERICAL SIMULATION

From the results of Liu et al., the HF-PSG etching speed for long times in a straight channel is diffusion limited. Experimental observations from the current test chips showed the HF-PSG interface propagates radially for a square structure with etch windows at each corner. Hence, the 1-D diffusion equation (with the appropriate boundary conditions) in radial coordinates was used to find the HF-PSG interface propagation speed. For comparison to the numerical results, experimental etch rate data were collected for the 400μm×400μm square geometries as shown in Figure 1.

The Radial Diffusion Equation

From experimental observations, the interface propagation appears axisymmetric, therefore, θ dependence of the diffusion equation can be neglected. In reality, the boundary conditions prevent the problem from being truly axisymmetric because no mass flux exits or enters the confining borders of the square geometries. Ignoring the z dependence, the diffusion equation in cylindrical coordinates[12] becomes:

$$\frac{\partial C}{\partial t}+V_r\frac{\partial C}{\partial r}=D\left(\frac{\partial^2 C}{\partial r^2}+\frac{1}{r}\frac{\partial C}{\partial r}\right) \qquad (1)$$

where C is the HF concentration, D is the diffusion coefficient, and V_r is the backflow velocity in the radial direction.

In order to simplify the above governing continuity equation, the magnitude of the convective term was compared to the diffusive term (see Liu et al.). The change in volume of the liquid at the etch front is examined by comparing the decrease of solid SiO_2 volume versus the increase of liquid H_2O volume. Thus a convective backflow velocity can be calculated and used to compare the convective and diffusive terms in

Eq. 1. Analyzing the experimental data from etching the square geometries, as indicated in Figure 4, the convective term is ~2 orders of magnitude lower than the diffusive term. In fact, if an order-of-magnitude analysis is performed, as in the straight channel analysis (see Liu et al.), the convective term in Eq. 1 will only become significant compared to the diffusive terms when the etch front is >3cm from the etch window. Therefore, the diffusion equation becomes:

$$\frac{\partial C}{\partial t} = D\left(\frac{\partial^2 C}{\partial r^2} + \frac{1}{r}\frac{\partial C}{\partial r}\right) \qquad (2)$$

subject to the Dirichelet boundary condition:

$$C(0,t) = C_b \qquad (3)$$

and the Neumann boundary condition:

$$\frac{\partial C(R(T),t)}{\partial r} = H(t) \qquad (4)$$

with the initial condition given as:

$$C(r,0) = C_0(r) \qquad (5)$$

In Eq. 3 C_b is the HF concentration of the bulk solution. In Eq. 4 $R(t)$ is the interface location measured from the origin and $H(t)$ is the flux at the interface as a function of time.

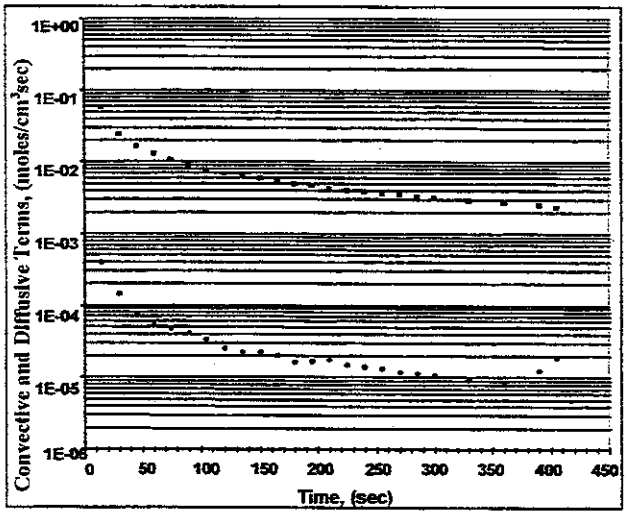

FIGURE 4: *Comparison of convective and diffusive terms in the mass diffusion equation. For this problem, the convective term is two orders of magnitude lower than the diffusive term and can be neglected.*

The Numerical Simulation

Selection of the Numerical Scheme

Depending on the desired accuracy and required computational time, various numerical schemes are available to solve the simple radial diffusion equation. The stability number S is often used to determine the stability of a numerical scheme and is defined below for a diffusive type equation:

$$S \equiv \frac{D\Delta t}{(\Delta r)^2} \qquad (6)$$

where Δt is the temporal increment and Δr is the spatial grid resolution. The Forward-in-Time-Center-in-Space[12] (FTCS) scheme is very simple to implement but it requires S to be less or equal to 0.5 for stability. If the simulation incremental time step (Δt) is set to 1sec then the spatial increment (Δr) must be greater than 56.6μm for this scheme to be stable given a diffusion coefficient of 1.6×10^{-5} cm²/sec (the diffusion coefficient was obtained from Liu et al.). This makes the spatial resolution of the simulation unacceptable. Conversely, if the spatial resolution of 1μm is desired, then the temporal step must be set less than 3×10^{-4}sec. This means that more than ~1×10^{6} time steps are required to complete a typical required simulation time of 6min to etch radially 200μm of PSG. Obviously, the FTCS scheme is not the scheme of choice. The Dufort-Frankel scheme is stable for $S>0$ and accurate to $O(\Delta r^2)$ but for consistency, Δt must be $<<\Delta r$. A 3-level explicit scheme can be formulated but requires fine grid spacing. Although the Crank-Nicolson scheme is more accurate than the Fully-Implicit scheme by an order in time and is unconditionally stable, it is mathematically more complicated and may have oscillating solutions on the border of unconditional stable region[13]. Hence, the Fully-Implicit scheme was used to solve Eq. 2.

The discretized radial diffusion equation using the Fully-Implicit scheme can be derived as:

$$C_j^n = S\left(\frac{\Delta r}{2R_j} - 1\right)C_{j-1}^{n+1} + (2S+1)C_j^{n+1} - S\left(\frac{\Delta r}{2R_j} + 1\right)C_{j+1}^{n+1} \qquad (7)$$

where n counts the temporal nodes, j counts the spatial nodes, and R_j is the distance from the origin to the *jth* node. The Neumann boundary condition for this scheme can be derived as:

$$C_J^{n+1} = \left(1/f_2\right)\left\{C_J^n + (f_1 + f_3)C_{J-1}^{n+1} - 2\Delta r f_3 H^{n+1}\right\} \qquad (8)$$

where

$$f_1 \equiv \left(S\left(\frac{\Delta r}{2R} - 1\right)\right) \quad f_2 \equiv (2S+1) \quad f_3 \equiv \left(S\left(-\frac{\Delta r}{2R} - 1\right)\right) \qquad (9)$$

The Thomas Algorithm[14] (Gauss Elimination) was used to solve Eq. 7 numerically. A novel *moving grid* procedure was devised to account for the time dependence of R_j and H^n when the diffusion equation is solved, making the prediction of the interface location as a function of time possible. The procedure is described below.

Algorithm for Solving the Etch rate

Since for short times the HF-PSG etch rate is

reaction-limited as shown in the straight channel analysis, then, for a small etch distance from the etch window, the etch rate of PSG in HF can be postulated to be independent of geometry. Thus for $R(t)$ small, the etch rate for the square PSG slab can be theorized to be equal to the reaction-limited etch rate of the straight channels. Consequently, the Neuman boundary condition for small $R(t)$ can be stipulated using Eq. 8 with H defined as:

$$H \equiv \frac{-6\rho}{DW}\left(\frac{d\delta}{dt}\right) \qquad (10)$$

where ρ is the PSG density, D is the diffusion coefficient of HF, W is the PSG molecular weight and $d\delta/dt$ is the initial etch rate obtained from Liu et al. In addition, the diffusion of fresh HF from the bulk solution occurs instantaneously to the PSG-HF interface for small $R(t)$, thus, the initial condition for all spatial nodes can be specified as C_b to start the simulation. This initial condition is applied to 10 nodes which represents R = 1μm. The required simulation time for the interface to move from R = 0 to R = 1μm is calculated as T_o = 1μm/$(d\delta/dt)$. The concentration profile in the square geometry, exactly T_o after the HF begins to etch the PSG slab, can be solved using the above assumption. After T_o, the concentration profile in the slab is known, including the concentration at the interface C_s which is equal to C_J. The simulation then advances spatially by Δr and assigns C_s as the initial concentration value of the new grid point, and use the profile at T_o as the initial condition for other grid points. Now, since C_J is known, the Neuman boundary condition can be found as

$$H \equiv \left(\frac{-1}{D}\right)\left(K_1 C_J + K_2 C_J^2\right) \qquad (11)$$

where K_1 and K_2 are the reaction constants determined by Liu et al. In addition, the new time of propagation is calculated as $\Delta t = \Delta r/(dR/dt)$. The etch rate dR/dt at this Jth nodal location (which corresponds to a time) can be calculated as:

$$\frac{dR}{dt} = H\left(\frac{-DW}{6\rho}\right) \qquad (12)$$

After Δt is reached, the spatial grid again advances by Δr and the Neuman boundary condition is updated again by Eq. 11. The simulation runs until R = 200μm, when the interfaces of the four etching fronts intersect and the diffusion equation becomes no longer valid.

The moving boundary procedure and the scheme used to update the time dependent flux at the boundary is graphically illustrated in Figure 5. A flow chart for the implementation of this procedure is shown in Figure 6. The algorithm was implemented in C programming language and takes ~30sec on a Sun SPARC 10 station to simulate a 200μm etch length with 1μm spatial resolution.

ANALYSIS OF THE EXPERIMENTAL AND NUMERICAL RESULTS

HF concentrations of 3.6, 26.0, 38.2 and 49.0% were used to etch the square geometries. The propagation of the interface is radial from the etch windows as shown in

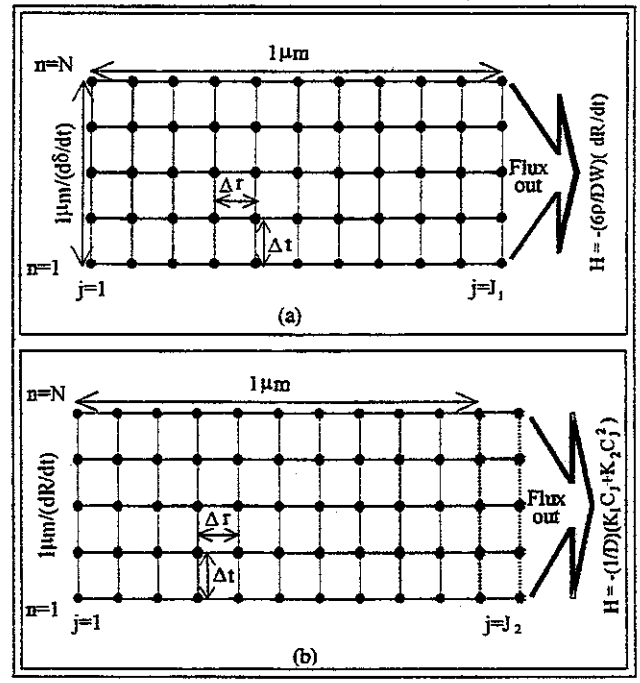

FIGURE 5. *(a) For $t<=T_o$, R=1μm, the reactive flux is calculated from 1-D results. (b) For $t>T_o$, R increments by Δr and the reactive flux is updated from the simulated interface concentration.*

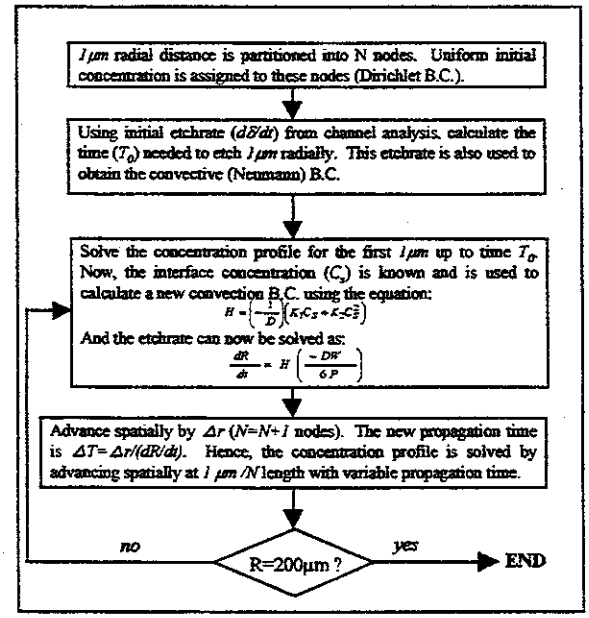

FIGURE 6. *Flow chart for implementing the moving boundary procedure.*

Figure 7 which also shows the simulated results in dashed lines. Experimental data for different concentrations of HF are compared with simulated results in Figure 8 and Figure 9. The experimental data shown in Figure 8 for each HF concentration are the averaged data from 5 different test structures (each test structure has 4 sets of data from 4 different etchwindows). The averaged data shown in Figure 9 are from 2 test structures, or a total of 8 sets of experimental data.

Discussion on the Etch rate

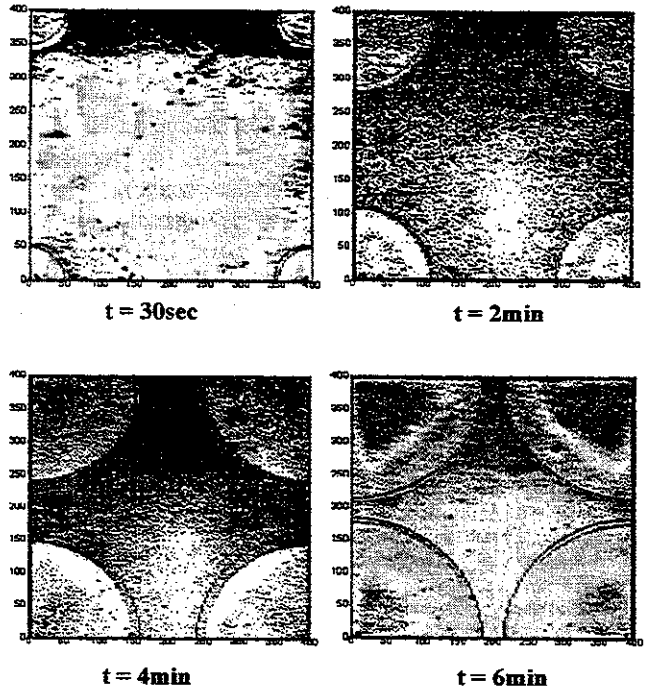

FIGURE 7. *Comparison of numerical and experimental results for 400×400μm sacrificial PSG etched in 49.0% HF. The dashed lines are the numerical results that are superimposed on time-lapsed video images from in-situ monitoring. Note the non-uniform interface propagation speed for the four corners which can be attributed to the non-uniform locale of the etch windows.*

Based on the experimental and simulated results several conclusions can be drawn on the HF-PSG etching mechanism. First, the initial etching mechanism is reaction dominated and is independent of device geometry. Second, as time progresses the etching phenomenon becomes diffusion limited, thus the interface propagation speed can be predicted by solving the appropriate continuity equation for a given device geometry. For the current study, sacrificial etching of square structures were characterized universally for different HF concentration, similar to the accomplishments of Liu et al. for straight channels. The etch rate in a straight channel can be modeled by a closed form solution, while the etch rate in a square slab can be numerically simulated. With the etching mechanisms elucidated, moving boundary numerical schemes can be formulated to predict the HF-PSG etch rate for MEMS devices of more complicated geometries.

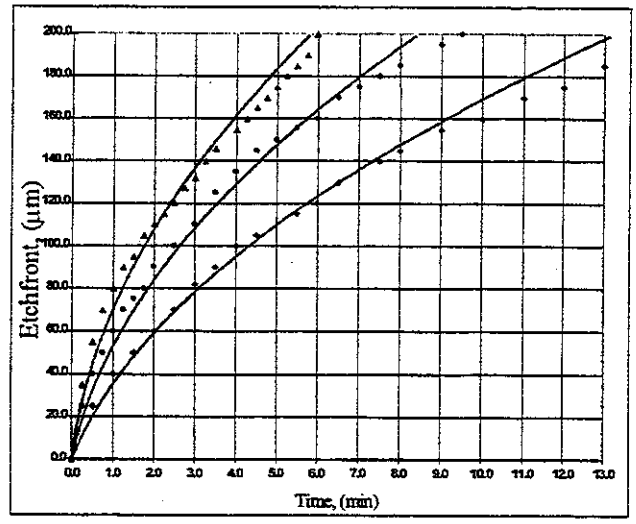

FIGURE 8. *The solid lines are the simulated etching front propagation as a function of time. The HF concentrations used are 49%, 38.2%, and 26%.*

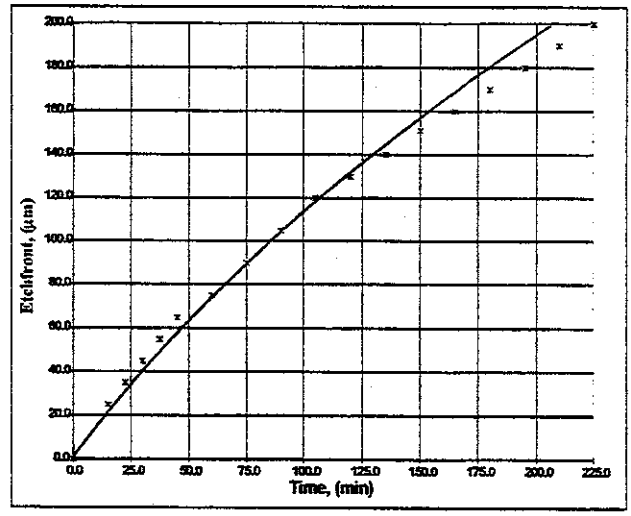

FIGURE 9. *Comparison of experimental and simulated results for HF concentration of 3.6%.*

The Diffusion Coefficient

From the numerical results, it was found that the diffusion coefficient was 4 times larger than the coefficient reported by Liu et al. This discrepancy can by explained readily by noting that the radial diffusion equation (Eq. 2) was solved with the assumption that the PSG-HF interface propagates in all angular directions. But for the square geometries, the physical PSG-HF interaction occurs only for $0°<\theta<90°$. Thus, physically, more HF molecules can be diffused to the interface for etching the PSG. Therefore, a higher diffusion coefficient is needed to compensate for the faster etching

speed.

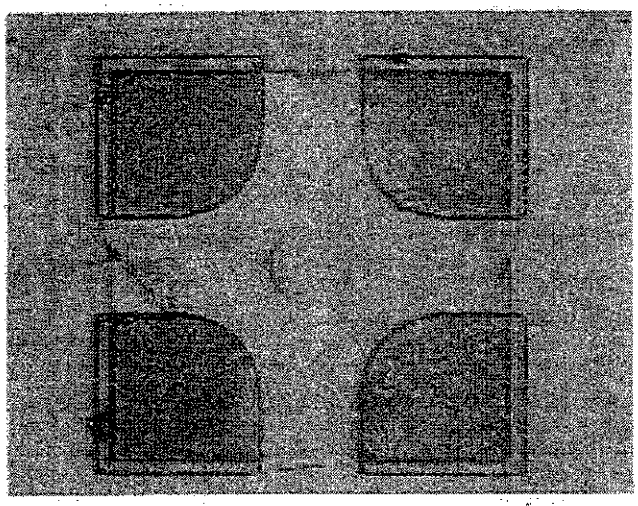

FIGURE 10. *The test structure used to validate the diffusion coefficient difference between the straight channel and square geometry analyses*

This further validates the postulate that the etching mechanism is diffusion limited, i.e., if an etch hole is placed at the center of a square diaphragm the same diffusion coefficient from the straight channel case can be used to solve the radial diffusion equation. An experimental structure on the same batch of chips was used for the verification of the aforementioned assertion. This is the square structure shown in Figure 10, which has a large circular etch hole of about 25μm at its center and etch openings along pad of its edges. The simulated results using 2 different diffusion coefficients along with the experimental result for this test structure are compared in Figure 11. Due to the larger etch window, the interface propagation of this structure was initially faster than the simulated result (solid line) obtained using the diffusion coefficient reported by Liu et al. But as time increases, the etching process becomes diffusion limited and the experimental etch rate approaches that of the modeled etch rate.

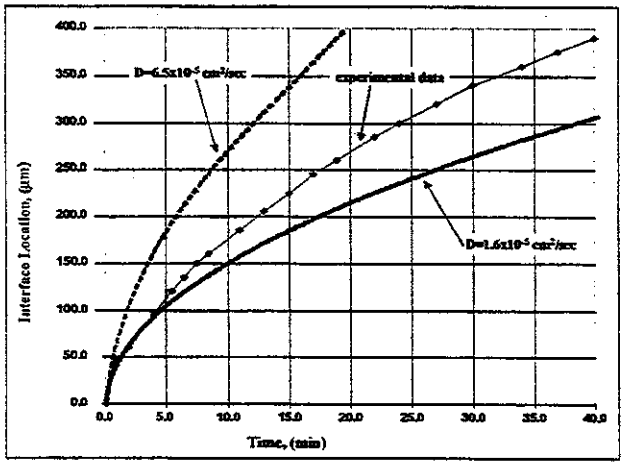

FIGURE 11. *Etch rate dependence on the diffusion coefficient.*

CONCLUSION

The physical mechanisms governing the sacrificial etching of PSG by HF was elucidated from an analysis of straight channel and square geometry structures. Sacrificial PSG was etched using concentrated HF acid and monitored in-situ. The two physical mechanisms, reaction and diffusion, which affect the etch rate of PSG in HF were studied. The etch rate of square PSG sacrificial layers were studied and characterized universally. The etch rate in a straight channel can be modeled by a closed form solution, while the etch rate in a square slab can be numerically simulated. Based on current results, the multidimensional diffusion equation can be used to predict the speed of sacrificial PSG etching by HF for more complicated geometries. As in the straight channel experiments, the etch rate also depends on the PSG thickness. This phenomenon is currently under investigation.

REFERENCES

1. Fan, L.S., Y.C. Tai and R. S. Muller, IEEE Transcript on Electron Devices, Vol. ED-35, No. 6, p. 724-730, 1988.
2. K. S. J. Pister, et al., *Microfabricated Hinges*, Sensors and Actuators A, 33, 249-256, 1992.
3. C. H. Mastrangelo, X. Zhang, and W. C. Tang, *Surface Micromachined Capacitive Differential Pressure Sensor with Lithographically-Defined Silicon Diaphragm*, The 8th International Conference on Solid-State Sensors and Actuators, Eurosensor IX, Stockholm, Sweden, June 25 - 29, 1995.
4. A. Gautier and P. Clausmann, Computer Rend., Vol. 157, Pp. 176, 1913.
5. A. Blumberg, J. Physical Chemistry, Vol. 63, Pp. 1129-1132, 1959.
6. J. S. Judge, *Solid State Science*, Journal of the Electrochemical Society., Pp. 1772-1775, November 1971.
7. W. E. Kline and H. S. Fogier, *Industrial Engineering Chemical Fundamentals*, Vol. 20, Pp. 155-161, 1981.
8. T. A. Lober and R. T. Howe, IEEE Solid-State Sensors and Actuators Workshop, IEEE Hilton Head Island, SC, Pp. 59-62, 1988.
9. D. J. Monk, et al., International Conference on Solid-State Sensors and Actuators: Transducers '91, IEEE, San Francisco, CA, Pp. 647-650, 1991.
10. D. J. Monk, et al., IEEE Solid-State Sensors and Actuators Workshop, Hilton Head Island, SC, Pp. 46-49, 1992.
11. J. Liu, et al., *In-Situ Monitoring and Universal Modeling of Sacrificial PSG Etching Using Hydroflouric Acid*, IEEE 0-7803-0957-2/93, 1993.
12. H. S. Carslaw and J. C. Jaeger, *Conduction of Heat in Solids*, 2nd Edition, Oxford at the Clarendon Press, 1959.
13. C. A. J. Fletcher, *Computational Techniques for Fluid Dynamics, Vol. I*, Springer-Verlag, 1988.
14. W. H. Press et al., *Numerical Recipes in C*, Cambridge University Press 1991.
15. K. Vanheusden and A. Stesmans, *Chemical Etch Rates in HF Solutions as a Function of Thickness of Thermal SiO2 and Buried SiO2 Formed by Oxygen Implantation*, Journal of Applied Physics, 69(9), May 1991.
16. H. Kikuyama, et al., *Etching Rate and Mechanism of Doped Oxide in buffered Hydrogen Fluoride Solution*, Journal of Electrochemical Society, Vol. 139, No. 8, August 1992.